JOURNAL OF GEOPHYSICAL RESEARCH, VOL. 101, NO. B2, PAGES 3113–3124, FEBRUARY 10, 1996

Nonlinear elasticity and stress-induced anisotropy in rock

P. A. Johnson[1]
Earth and Environmental Sciences Division, Los Alamos National Laboratory, Los Alamos, New Mexico

P. N. J. Rasolofosaon
Institut Français du Pétrole, Rueil Malmaison, France

Abstract. The elastic nonlinear behavior of rocks as evidenced by deviations from Hooke's law in stress-strain measurements, and attributable to the presence of mechanical defects (compliant features such as cracks, microfractures, grain joints), is a well-established observation. The purpose of this paper is to make the connection between the elastic nonlinearity and stress-induced effects on waves, in this case uniaxial-stress-induced transverse isotropy. The linear and nonlinear elastic coefficients constitute the most condensed manner in which to characterize the elastic behavior of the rock. We present both the second- and the third-order nonlinear elastic constants obtained from experimental data on rock samples assumed homogeneous and isotropic when unstressed. As is normally the case, the third-order (nonlinear) constants are found to be much larger than the second-order (linear) elastic constants. Contrary to results from intact homogeneous solids (materials without mechanical defects), rocks exhibit weak to strong nonlinearity and always in the same manner (i.e., an increase of the moduli with pressure). As a consequence the stress-induced P wave anisotropy and S wave birefringence can be large. The stress-induced P wave anisotropy appears to be much larger than the S wave birefringence. The fast direction is parallel to the stress direction, and the anisotropy goes as $\sin^2\theta$, θ being the angle between the propagation direction and the stress direction. Experiments on rocks indicate that at low applied stresses, the proportionality of the stress and the induced S birefringence and P anisotropy predicted by theory is well corroborated.

Introduction

The nonlinear elastic response of rock is a well-established, now classical observation. For example, one well-known manifestation of elastic nonlinearity is the dependence of the elastic properties or rocks on applied stress as demonstrated by countless laboratory experiments [e.g., *Birch*, 1966]. Another well-known observation in both the laboratory and in the Earth is the anisotropic nature of rock and of the stress fields [e.g., *Zoback*, 1992]. In this work we intend to show how elastic nonlinearity and elastic anisotropy are connected and how the nonlinear response varies with anisotropy, and vice versa.

Nonlinear elasticity in rock is due to the presence of compliant mechanical defects (cracks, microfractures, grain joints) [e.g., *Walsh*, 1965; *Jaeger and Cook*, 1979; *Bourbié et al.*, 1987]. Many recent experiments in rocks show strong nonlinear elastic wave response, much larger than that of gases, liquids, or most other solids [e.g., *Meegan et al.*, 1993; *Johnson et al.*, 1993; *Johnson and McCall*, 1994]; however, relatively few measurements exist on rocks of the complete set of higher-order elastic constants that describe elastic nonlinear behavior [*Bakulin and Protosenya*, 1982; *Nazarov et al.*, 1988]. In this paper we will describe measurements of nonlinear constants in rocks from wave propagation experiments and calculation of these constants from data available in the literature. We will then show the connection between these nonlinear parameters and frequently measured experimental parameters such as the stress-induced P wave anisotropy, the S wave birefringence, and the relative variations of P and S wave velocity ratio $\gamma = V_P/V_S$. Shear wave splitting, quantified by the S birefringence, has long been recognized as diagnostic of seismic anisotropy in the Earth's crust but also provides information regarding the in situ crack and stress structure of rock masses, leading to potential industrial applications (see review by *Crampin and Lovell* [1991]). The ratio γ contains information on the lithologic type and the physical state of rocks [e.g., *Pickett*, 1963].

We shall first review the classical theory of wave propagation in nonlinear elastic media. We then deduce the expressions of the P wave anisotropy and the S wave birefringence for transverse isotropy induced by uniaxial stress. This will be followed by the illustration of the effect of variations of γ as a function of the applied stress and the elastic constants. Finally, we shall apply the analysis to experimental data on rocks.

Fundamentals of Nonlinear Elastodynamics

The detailed development of the elastic nonlinear theory can be found in numerous textbooks [e.g., *Truesdell*, 1965; *Green*, 1973]. Here we summarize the general equations. (We note that there is mounting evidence indicating that the classical approach cannot necessarily be applied directly to rocks, especially at lower pressures [e.g., *McCall and Guyer*, 1994; *Guyer et al.*, 1995; P. A. Johnson et al., Resonance and elastic nonlinear phenomena in rock, submitted to *Journal of Geo-*

[1]Also at Department de Recherches Physiques, Université Pierre et Marie Curie, Paris.

Paper number 95JB02880.
0148-0227/96/95JB-02880$05.00

physical Research, 1995]. It may well be that the widely observed discrete memory effect in static tests must be accounted for in wave propagation as well.)

The equation of motion is

$$\rho\ddot{u}_i = \partial\sigma_{ij}/\partial x_j, \tag{1}$$

where ρ, σ, and $\ddot{u}$ designate the density, the stress tensor, and the particle acceleration, respectively. Einstein's summation convention on repeated indices is assumed. The stress tensor is given by

$$\sigma_{ij} = \frac{\partial E}{\partial(\partial u_i/\partial x_j)}, \tag{2}$$

where E designates the elastic strain energy, which, developed to the third order in strain ε in a general elastic medium, is [*Brugger*, 1964]

$$E = \tfrac{1}{2}C_{ijkl}\varepsilon_{ij}\varepsilon_{kl} + \tfrac{1}{6}C_{ijklmn}\varepsilon_{ij}\varepsilon_{kl}\varepsilon_{mn}, \tag{3}$$

where C_{ijkl} and C_{ijklmn} designate the components of the second-order elastic (SOE) tensor and the third-order elastic (TOE) tensor, respectively. The complete set of SOE and TOE constants is the most condensed manner in which to summarize the linear and nonlinear elastic properties of a solid. The order of an elastic constant corresponds to the power of the corresponding strain ε in the development of the elastic strain energy E in (3). The SOE (or TOE) tensor exhibits the internal symmetries $C_{ijkl} = C_{jikl} = C_{ijlk} = C_{klij}$ (or $C_{ijklmn} = C_{jiklmn} = C_{ijlkmn} = C_{ijklnm} = C_{klijmn} = C_{mnklij}$) and is characterized by 21 (or 56) independent components in the lowest material symmetry (triclinic) and by 2 (or 3) in the highest symmetry (isotropic). The mechanical stability of the medium imposes that medium requires energy to undergo elastic deformation, which implies that each of the two terms in the right-hand side of (3) must be positive for any state of strain. This leads to six well-known constraints on the SOE constants [e.g., *Helbig*, 1994]. We are not aware of similar constraints published for the TOE constants.

In (3) the components of the Lagrangian strain tensor ε are given by

$$2\varepsilon_{ij} = \frac{\partial u_i}{\partial x_j} + \frac{\partial u_j}{\partial x_i} + \frac{\partial u_k}{\partial x_i}\frac{\partial u_k}{\partial x_j}. \tag{4}$$

By inserting (2) into (1) and using (3) and (4), one obtains the general nonlinear elastodynamic equation

$$\rho\ddot{u}_i = \frac{\partial^2}{\partial x_j \partial x_l}\left[C_{ijkl} + (C_{ijklmn} + C_{ijlm}\delta_{kn} + C_{ilnm}\delta_{jk} + C_{iklm}\delta_{jn})\frac{\partial u_m}{\partial x_n}\right]u_k, \tag{5}$$

where δ is the Kronecker symbol. In the case of small displacements the third term of the right-hand side of (4) can be neglected, and one finds the classical linear relation between the strain and displacement. However, when dealing with finite deformation, (4) is nonlinear. This nonlinearity is of a "geometrical" or "kinematic" type and is related to the difference between the Lagrangian and Eulerian descriptions of motion [*Zarembo and Krasil'nikov*, 1971]. The nonlinearity remains even if the TOE constants C_{ijklmn} in (3) vanish, thus explaining the presence of the nonlinear term $(C_{ijlm}\delta_{kn} + C_{ilnm}\delta_{jk} + C_{iklm}\delta_{jn})$ in the general nonlinear elastodynamic equation (5).

The other type of elastic nonlinearity is "physical" nonlinearity. Physical nonlinearity is contained in the TOE coefficients C_{ijklmn} (equations (3) and (5)) and accounts for the fact that stress is no longer a linear function of strain even for moderate to small strain levels (i.e., even if the strain-displacement relation (4) becomes linear). This is the case in materials exhibiting strong nonlinearity, such as rock.

In the particular case where the medium is isotropic, the elastic energy E in (3) simplifies to [*Murnaghan*, 1951]

$$E = \frac{\lambda + 2\mu}{2}I_1^2 - 2\mu I_2 + \frac{l + 2m}{3}I_1^3 - 2mI_1I_2 + nI_3, \tag{6}$$

where $\lambda = C_{12}$ and $\mu = C_{66}$ are the SOE constants (or Lamé parameters), $l = \frac{1}{2}C_{112}$, $m = \frac{1}{4}(C_{111} - C_{112})$ and $n = \frac{1}{2}(C_{111} - 3C_{112} + 2C_{123})$ are the TOE constants (Murnaghan coefficients), $I_1 = \varepsilon_{ii}$, $I_2 = \frac{1}{2}(\varepsilon_{ii}\varepsilon_{jj} - \varepsilon_{ij}\varepsilon_{ji})$, and $I_3 = \det(\varepsilon_{ij})$ [e.g., *Zarembo and Krasil'nikov*, 1971].

Nonlinear Acoustics and Acoustoelasticity

Two cases are generally considered in the literature on wave propagation in nonlinear elastic media. The first case is that of the nonlinear acoustics community [e.g., *Zarembo and Krasil'nikov*, 1971; *Hamilton*, 1986], in which waves are considered finite in amplitude and velocities depend on the strain level. As a consequence, an initially sinusoidal waveform will not maintain its shape during propagation in the absence of large dissipation because the wave crests overtake the wave troughs, leading ultimately to a shock wave [e.g., *Gol'dberg*, 1957]. For a P wave propagating in a one-dimensional (1-D) isotropic medium,

$$V_P(\varepsilon) \approx V_P(\varepsilon = 0)(1 - \beta\varepsilon), \tag{7}$$

where $V_P(\varepsilon = 0)$ and $V_P(\varepsilon)$ denote the linear and the nonlinear velocities, respectively. The nonlinear acoustic coefficient β is given by

$$\beta = \frac{3}{2} + \frac{l + 2m}{\lambda + 2\mu}. \tag{8}$$

Note that the magnitude of the nonlinear response is quantified not by the absolute value of the TOE constants but by the ratio between the TOE and the SOE constants.

A second nonlinear elastic case corresponds to a small wave perturbation superimposed on a static predeformation due to the presence of a static prestress. This is the field of acoustoelasticity [e.g., *Pao et al.*, 1984], which is the acoustical analog of photoelasticity in optics. *Thurston and Brugger* [1964] have analyzed two such cases, namely, uniaxially and hydrostatically prestressed anisotropic media. In the case of uniaxial prestress the stress derivative of the wave modulus is given by

$$\left(\frac{\partial(\rho_0 W^2)}{\partial\sigma}\right)_{\sigma=0} = -(\mathbf{n}\cdot\mathbf{m})^2 - 2wF - H, \tag{9}$$

where W is the "natural" velocity (i.e., the length of the "acoustical path" in the unstressed state divided by the wave travel time in the stressed state), ρ_0 is the density in the unstressed state, and $\mathbf{n}$ and $\mathbf{m}$ are the unit vectors in the directions of wave propagation in the unstressed state and of the uniaxial stress, respectively.

In the case of a uniaxial prestress, the quantities w, F, and H are given by

$$w = C^S_{ijkl} n_i n_k p_j p_l, \tag{10a}$$

$$F = S^T_{ijkl} m_i m_j p_k p_l, \tag{10b}$$

$$H = S^T_{ijkl} C_{kltrsq} m_i m_j n_t n_s p_r p_q, \tag{10c}$$

where C^S and S^T are the SOE isentropic stiffness and isothermal compliance tensors, respectively, of the unstressed medium and p_j are the components of the unit polarization vector of the wave in the unstressed state.

In the case of an applied hydrostatic prestress, the term $(\mathbf{n} \cdot \mathbf{m})^2$ in (9) is replaced by 1. In this case, w, F, and H are given by

$$w = C^S_{ijkl} n_i n_k p_j p_l, \tag{11a}$$

$$F = S^T_{iirs} p_r p_s, \tag{11b}$$

$$H = S^T_{iiuv} C_{uvprqs} n_p n_q p_r p_s. \tag{11c}$$

Here the symmetry of the stressed medium is entirely determined by the symmetry of the SOE and the TOE tensors, which have the same symmetry as the unstressed medium. As a consequence, the elastic symmetry is unchanged under hydrostatic stress. Note that the tensor C^S can be identified with the fourth-rank tensor C in (3) and that w is the wave modulus in the unstressed state. Also, as was noted by *Green* [1973], for practical applications a major advantage of (9) is that all the physical parameters involved are evaluated in the unstressed state ($\sigma = 0$) and as a consequence do not involve stress-induced changes in the symmetry of the medium. Note also that in materials having C_{ijklmn} values much larger than C_{ijkl} values, the physical nonlinear term H will be much more important than the geometrical nonlinear term $2wF$ in (9) to (11). This is the case in strongly nonlinear materials such as rocks, as will be illustrated below.

In the case of the most general state of prestress (triclinic), the stress tensor σ can be decomposed in three eigenstresses $\sigma = (\sigma^{(\mathrm{I})}(\mathbf{m}^{(\mathrm{I})}), \sigma^{(\mathrm{II})}(\mathbf{m}^{(\mathrm{II})}), \sigma^{(\mathrm{III})}(\mathbf{m}^{(\mathrm{III})}))$, where the $\sigma^{(i)}(\mathbf{m}^{(i)})$ (i = I, II, III) are uniaxial mutually perpendicular stresses in directions of unit vectors $\mathbf{m}^{(i)}$. The first-order Taylor expansion of the stressed modulus $M(\sigma)$ around zero stress is

$$M(\sigma) = M(\sigma = 0) + \left(\frac{\partial M}{\partial \sigma^{(\mathrm{I})}}\right)_{\sigma=0} \sigma^{(\mathrm{I})} + \left(\frac{\partial M}{\partial \sigma^{(\mathrm{II})}}\right)_{\sigma=0} \sigma^{(\mathrm{II})} + \left(\frac{\partial M}{\partial \sigma^{(\mathrm{III})}}\right)_{\sigma=0} \sigma^{(\mathrm{III})}, \tag{12}$$

where $M(\sigma = 0)$ is the wave modulus in the unstressed medium and $(\partial M/\partial \sigma^{(i)})_{\sigma=0}$ (i = I, II, III) are given by (9) and (10). In theory, (12) can be applied if the stress is not too large, that is to say, as long as $|M(\sigma) - M(\sigma = 0)| \ll |M(\sigma = 0)|$. This is fulfilled if $|\partial M/\partial \sigma||\sigma| \ll |M(\sigma = 0)|$. From (9) and (10) this can be reduced to the condition

$$\sigma_{ij}^2 C'^2_{ijklmn} \ll (C'^2_{ijkl})^2. \tag{13}$$

We assume in (10), (11), and (13), as in the rest of the paper, that the isothermal stiffness tensor C^T (or compliance tensor S^T) does not differ much from the isentropic stiffness tensor C^S (or compliance tensor S^T). Their difference is of the same order as or smaller than the combined deviations due to errors of measurements of these constants and the variability of the elastic properties in the material [*Hearmon*, 1961]. Condition (13) summarizes the domain of validity of (12). Note that (12) is a very general equation. The equation gives the stress dependence of the modulus of an arbitrary wave (qP, $qS1$ or $qS2$) propagating in any direction of a homogeneous, anisotropic medium of arbitrary symmetry, submitted to an arbitrary (but uniform) static prestress.

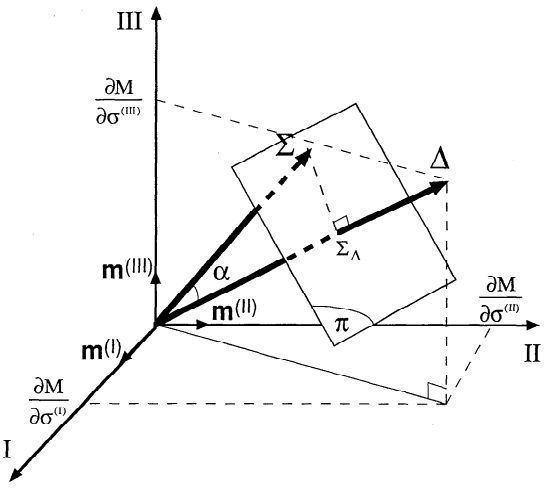

Figure 1. Geometrical interpretation of equation (12) and representation in the eigenstress axes (I, II, III) of the isovelocity/isomodulus plane π perpendicular to the gradient vector $\mathbf{\Delta}$ and defined by the loci of the extremity of the stress vector $\mathbf{\Sigma}$.

For fixed eigendirections of stress $\mathbf{m}^{(i)}$ (i = I, II, III) and for a given wave and propagation direction (i.e., $\mathbf{n}$ and $\mathbf{p}$ fixed in (9) and (10)), (12) has a simple geometrical interpretation. This is illustrated in Figure 1. In the coordinate system (I, II, III) aligned with the vectors $\mathbf{m}^{(i)}$ (i = I, II, III), the stress σ can be represented by the vector $\mathbf{\Sigma}$ of components $(\sigma^{(\mathrm{I})}, \sigma^{(\mathrm{II})}, \sigma^{(\mathrm{III})})$. If one introduces the gradient vector $\mathbf{\Delta}$ of components $(\partial M/\partial \sigma^{(\mathrm{I})}, \partial M/\partial \sigma^{(\mathrm{II})}, \partial M/\partial \sigma^{(\mathrm{III})})$, the quantity $(\partial M/\partial \sigma^{(\mathrm{I})})_{\sigma=0}\sigma^{(\mathrm{I})} + (\partial M/\partial \sigma^{(\mathrm{II})})_{\sigma=0}\sigma^{(\mathrm{II})} + (\partial M/\partial \sigma^{(\mathrm{III})})_{\sigma=0}\sigma^{(\mathrm{III})}$ is equal to the scalar product $\mathbf{\Sigma} \cdot \mathbf{\Delta}$. Thus the states of stress that keep the moduli (or the velocities) constant are represented by vectors $\mathbf{\Sigma}$ that have a constant projection Σ_Δ along $\mathbf{\Delta}$. The extremity of the vectors $\mathbf{\Sigma}$ are contained in a plane π perpendicular to $\mathbf{\Delta}$. We refer to this plane as an isovelocity or isomodulus stress plane. In the particular case of an initially isotropic medium one has $\partial M/\partial \sigma^{(\mathrm{I})} = \partial M/\partial \sigma^{(\mathrm{II})} = \partial M/\partial \sigma^{(\mathrm{III})}$, which implies that the isovelocity stress plane is normal to the direction (1, 1, 1).

We conclude with some symmetry considerations. The symmetry principles stated by *Nur* [1971] are contained in (9), (12), (14), (15), and (16) and are direct consequences of a very general principle outlined by P. Curie [e.g., *Curie*, 1894; *Curie*, 1955; *Sirotine and Chaskolskaya*, 1975] regarding the influence of symmetry on physical phenomena. The principle states that effects are at least as symmetric as their causes. The corollary is that if the effects lack a symmetry element, so do their causes. In other words, the symmetry group of the causes (i.e., the unstressed medium and the stress field in our case) is a subgroup of the symmetry group of the effects (i.e., the stressed medium in our case). For example, the symmetry group of an initially isotropic medium under an arbitrary (but uniform) stress field is orthorhombic, and thus such a stressed medium is of at least the same symmetry. In other words, orthorhombic symmetry is the lowest level of symmetry that can be exhibited by an initially isotropic medium uniformly submitted to an arbitrary state of stress. Another example is an initially orthor-

hombic medium that is uniaxially stressed. Such a medium is orthorhombic, monoclinic, or triclinic if the stress is perpendicular to a symmetry plane, contained in a symmetry plane, or out of any of the three symmetry planes, respectively. Similar results can be easily deduced using this principle in the case of media and/or prestress belonging to other symmetry groups.

Stress-Induced Anisotropy in Initially Isotropic Media

In the particular case of an initially isotropic medium and vertical uniaxial prestress, the resulting symmetry is transverse isotropy with a vertical symmetry axis. The parameters w, F, and H in (9) become the following: for the P wave,

$$w_P = C_{11} = \lambda + 2\mu, \tag{14a}$$

$$F_P = S_{11}c^2 + S_{12}s^2, \tag{14b}$$

$$H_P = C_{111}(S_{11}c^2 + S_{12}s^2) + C_{112}(S_{11}s^2 + 2S_{12}c^2); \tag{14c}$$

for the SV-wave (i.e., the S wave polarized in the plane defined by the direction of propagation and the direction of the applied uniaxial stress),

$$w_{SV} = C_{66} = \mu, \tag{15a}$$

$$F_{SV} = S_{11}s^2 + S_{12}c^2, \tag{15b}$$

$$4H_{SV} = C_{111}(S_{11} + S_{12}) + C_{112}(S_{12} - S_{11}) - 2C_{123}S_{12}; \tag{15c}$$

and for the SH-wave (i.e., the S-wave polarized normal to the plane defined by the direction of propagation and the direction of the applied uniaxial stress),

$$w_{SH} = C_{66} = \mu, \tag{16a}$$

$$F_{SH} = S_{12}, \tag{16b}$$

$$4H_{SH} = C_{111}(S_{11}c^2 + S_{12}s^2 + S_{12}) + C_{112}[S_{11}(2 - 3c^2) + S_{12}(1 + s^2)] - 2C_{123}(S_{11}s^2 + S_{12}c^2). \tag{16c}$$

In (14), (15), and (16) we adopted Voigt's contracted index notation convention for the components of all the elastic tensors [e.g., *Brugger*, 1964]. The quantities $c^2 = (\mathbf{n} \cdot \mathbf{m})^2 = \cos^2\theta$ and $s^2 = \sin^2\theta$ are directional parameters, where θ is the angle between the direction of propagation and the direction of the uniaxial stress. Note that the F terms in (14) and (15) have elliptical dependence on θ, the w terms are independent of θ, and H is independent of θ in (15) and has elliptical dependence in (14). The compliance coefficients are given by

$$S_{66} = \frac{1}{C_{66}}, \qquad S_{11} = \frac{C_{11} + C_{12}}{(C_{11} - C_{12})(C_{11} + 2C_{12})}, \tag{17}$$

where $C_{12} = C_{11} - 2C_{66}$ and $S_{12} = S_{11} - S_{66}/2$.

In the case where the direction of propagation is either perpendicular or parallel to the direction of the applied stress, the expressions become simpler [*Hughes and Kelly*, 1953]. For example, in the case of a uniaxial stress σ in the direction of wave propagation, equations (9), (14), (15), and (16) become

$$\rho V_{P\parallel}^2 = \lambda + 2\mu - \frac{\sigma}{3K}\left[2l + \lambda + \frac{\lambda + \mu}{\mu}(4m + 4\lambda + 10\mu)\right], \tag{18a}$$

$$\rho V_S^2 = \mu - \frac{\sigma}{3K}\left(m + \frac{\lambda n}{4\mu} + 4\lambda + 4\mu\right), \tag{18b}$$

where $K = \lambda + \frac{2}{3}\mu$ is the unperturbed bulk modulus. When the direction of propagation is perpendicular to the direction of the uniaxial stress σ, the fast shear wave S_1 and the slow shear wave S_2 are polarized parallel and perpendicular to the stress direction, respectively. These velocities are given by

$$\rho V_{P\perp}^2 = \lambda + 2\mu - \frac{\sigma}{3K}\left[2l - \frac{2\lambda}{\mu}(m + \lambda + 2\mu)\right], \tag{19a}$$

$$\rho V_{S_1}^2 = \mu - \frac{\sigma}{3K}\left(m + \frac{\lambda n}{4\mu} + \lambda + 2\mu\right), \tag{19b}$$

$$\rho V_{S_2}^2 = \mu - \frac{\sigma}{3K}\left(m - \frac{\lambda + \mu}{2\mu}n - 2\lambda\right). \tag{19c}$$

Note that wave propagation in prestressed media is centrosymmetric because it involves only the even rank SOE and TOE tensors. Thus uniaxially stress-induced transverse isotropy implies a symmetry plane perpendicular to the direction of the uniaxial stress.

When hydrostatic stress p is exerted on the medium, the state of stress is equivalent to a state of stress with three uniaxial stresses of the same magnitude but oriented in three orthogonal directions. We can take one of these directions collinear to the direction of propagation and perpendicular to the two remaining directions of uniaxial stress. Thus using (18) and (19), the shear and the compressional velocities under hydrostatic pressure p are given by

$$\rho V_P^2 = \lambda + 2\mu - \frac{p}{3K}(6l + 4m + 7\lambda + 10\mu), \tag{20a}$$

$$\rho V_S^2 = \mu - \frac{p}{3K}(3m - \tfrac{1}{2}n + 3\lambda + 6\mu). \tag{20b}$$

Because the state of stress is isotropic, the initially isotropic medium remains isotropic and no directional dependence is observed in (20). In the case of fluids one has $\mu = 0$, $l = -\frac{1}{2}\lambda(5 + B/A)$, $m = -\lambda$ and $n = 0$, where A and B are the first two coefficients of the Taylor expansion of the equation of state of the medium [e.g., *Beyer*, 1972; *Kostek et al.*, 1993]. In this case the second equation of (20) vanishes, and the TOE nonlinearity is defined by only one coefficient, namely, l or B/A.

Relation Between Nonlinearity and Elastic Parameters

In this section we consider only waves in initially isotropic media. We restrict our discussion to hydrostatic prestress and to transverse isotropy induced by uniaxial stress. Our purpose here is to express the variations of elastic parameters such as the S wave birefringence and P wave anisotropy induced by an applied uniaxial stress. The only directional parameter for wave propagation is the angle θ between the direction of propagation and the direction of the uniaxial stress.

The S wave birefringence $B_S(\theta)$ is usually defined as

$$B_S(\theta) = \frac{V_{S_1}(\theta) - V_{S_2}(\theta)}{V_{S_1}(\theta)}, \tag{21}$$

where V_{S_1} and V_{S_2} are the velocities of the fastest and the slowest S wave, respectively. These velocities correspond in our case to the SV and the SH wave, respectively [e.g., *Leary et al.*, 1990]. Note that all the velocities depend on the angle of propagation θ, and as a consequence, B_S does as well. If the magnitude of the prestress is not too large, that is to say when condition (13) is fulfilled, using (9), (15), and (16), equation (21) gives

$$B_S(\theta) \approx -\frac{\sigma}{2\mu}[2\mu(F_{SV} - F_{SH}) + (II_{SV} - II_{SH})]$$

$$= -\sigma\frac{4\mu + n}{4\mu^2}\sin^2\theta = -\sigma b_S \sin^2\theta, \qquad (22)$$

where $w_{SH} = w_{SV} = \mu$, and where $b_S = (4\mu + n)/8\mu^2$ is an elastic parameter that we shall call the stress-induced S birefringence coefficient. In this particular case the condition (13) leads to $|\sigma| \ll \mu^2/|n|$, which is the condition of validity of (22). Note that the maximum birefringence occurs when $\theta = 90°$, that is to say, when both the S waves propagate in a direction perpendicular to the direction of the uniaxial stress. Note also that the birefringence is directly proportional to the stress σ and that the directional dependence of the S birefringence is simply contained in the function $\sin^2\theta$.

In a very similar manner one can define P wave anisotropy $A_P(\theta)$ by

$$A_P(\theta) = \frac{V_{P\|} - V_P(\theta)}{V_{P\|}}, \qquad (23)$$

where $V_{P\|}$ and $V_P(\theta)$ are the P wave velocities in the fastest direction, i.e., along the stress direction and in an arbitrary direction θ, respectively. As for B_S, the parameter A_P depends on the angle of propagation θ. If the magnitude of the prestress is not too large, that is to say, when condition (13) is fulfilled, using (9) and (14), equation (23) gives

$$A_P(\theta) \approx -\frac{\sigma}{2(\lambda + 2\mu)}[1 - \cos^2\theta + 2(\lambda + 2\mu)$$

$$\cdot (F_P(\theta = 0°) - F_P(\theta)) + (H_P(\theta = 0°) - H_P(\theta))]$$

$$= -\sigma\frac{2\lambda + 5\mu + 2m}{2\mu(\lambda + 2\mu)}\sin^2\theta. \qquad (24)$$

Here we have used the relation $w_P = \lambda + 2\mu$ (see (14)). Note that condition (13) for this particular case leads to $|\sigma| \ll \mu(|\lambda| + |\mu|)/|m|$, which is the condition of validity of (24). This last equation can thus be written,

$$A_P(\theta) = -\sigma\frac{2\lambda + 5\mu + 2m}{2\mu(\lambda + 2\mu)}\sin^2\theta = -\sigma a_P \sin^2\theta, \qquad (25)$$

where $a_P = (2\lambda + 5\mu + 2m)/[2\mu(\lambda + 2\mu)]$ is an elastic parameter that we shall call the stress-induced P wave anisotropy coefficient. As for S birefringence, note that the maximum P velocity deviation is between the propagation directions parallel and perpendicular to the direction of uniaxial stress, that the P wave anisotropy is directly proportional to the stress σ, and that the directional dependence is simply described by the function $\sin^2\theta$.

We can compute the variation of the parameter $\gamma(p) = V_P(p)/V_S(p)$ induced by the hydrostatic pressure p, because such data exist. We simplify $\gamma(p)$ in the following manner to compute the variation. If the magnitude of the hydrostatic prestress is not too large, that is, when condition (13) is verified, one has

$$\frac{\gamma(p)}{\gamma(p = 0)} \approx \frac{1 - \frac{1}{2}\zeta p}{1 - \frac{1}{2}\eta p} \approx 1 - \tfrac{1}{2}(\zeta - \eta)p, \qquad (26)$$

where

$$\zeta = \frac{6l + 4m + 7\lambda + 10\mu}{3K(\lambda + 2\mu)}, \qquad \eta = \frac{3m - \frac{1}{2}n + 3\lambda + 6\mu}{3K\mu},$$

and where $\zeta p \ll 1$ and $\eta p \ll 1$ (due to the condition prescribed in (13)). Thus (26) becomes

$$\frac{\Delta\gamma}{\gamma} = \frac{\gamma(p) - \gamma(p = 0)}{\gamma(p = 0)} \approx \tfrac{1}{2}(\eta - \zeta)p. \qquad (27)$$

Note that the last term describes a linear relationship between $\Delta\gamma/\gamma$ and p.

Experimental Data

Our aim here is not to present an exhaustive analysis of the experimental data available from the literature but to illustrate the relevance of the above analysis. We shall focus on data from rocks that can be considered as initially isotropic without applied stress. *Zamora* [1990] published data for "natural" and "thermally cracked" Fontainebleau sandstone F32 (porosity $\phi = 8.9\%$), both dry and water saturated, and dry marble D82 ($\phi = 0.8\%$). *Nur and Simmons* [1969] published data for dry Barre granite ($\phi = 0.6\%$). The influence of uniaxial stress on anisotropy was studied in both papers. Zamora considered wave propagation in two directions perpendicular to the direction of stress, whereas Nur and Simmons studied propagation in the entire plane containing the direction of stress. Data from *Lucet* [1989] using water-saturated Brauvilliers limestone ($\phi = 30.8\%$) under confining pressure will also be considered here.

One manner in which to check the validity and implications of the cubic development of the strain energy E in (3) is to plot the relative variations $[V_P^2(\sigma) - V_P^2(\sigma = 0)]/[V_P^2(\sigma = 0)]$ of the velocities as functions of the applied stress σ. This is done in Figure 2 for P waves in Fontainebleau sandstone. We can see that the proportionality between the relative velocity variations and the stress described by (19), plotted as solid lines in Figure 2, holds as long as the stress level is not too high. For higher pressures, higher-order elastic constants are required to describe the rock response. Following (18), (19), or (20), if three such curves are available on the same rock sample, as is the case with data from *Zamora* [1990] and *Nur and Simmons* [1969], it is possible to invert all the TOE constants.

We have adopted the following procedure to separately invert the SOE and TOE constants. Because the rocks are assumed to be initially isotropic, we first compute the averages of all the measured P wave and S wave unstressed moduli and assume that they are equal to the SOE constants $\lambda + 2\mu$ and μ, respectively. Then for each experimental plot of the wave modulus versus stress (as in Figure 2), we perform a linear regression on the first three or four points typically and identify the slope with $[\partial(\rho_0 W^2)/\partial\sigma]_{\sigma=0}$ in (9). Given the SOE constants and using (14), (15), or (16), we then compute the "corrected" slope $[\partial(\rho_0 W^2)/\partial\sigma]_{\sigma=0} + (\mathbf{n}\cdot\mathbf{m})^2 + 2wF$, which is a multilinear function H of the TOE constants (see (9) and (10)). Finally, the three TOE constants are inverted by

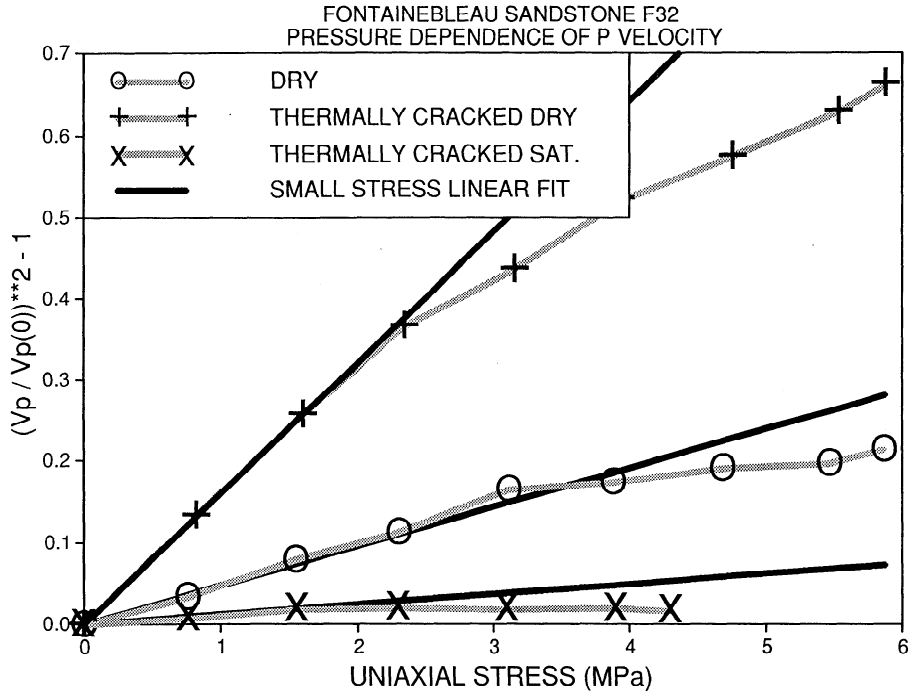

Figure 2. Relative variation $[V_P^2(\sigma) \quad V_P^2(\sigma = 0)]/[V_P^2(\sigma = 0)]$ of the P wave velocity as function of the uniaxial stress σ in "natural" and "thermally cracked" Fontainebleau sandstone, both dry and saturated. Direction of propagation is perpendicular to the applied stress. Experimental data are from *Zamora* [1990]. Theoretical results from equation (19) are shown as solid lines.

multilinear regression on all the available slope data. The accuracy of the velocities is better than 2% for *Nur and Simmons* [1969], and is around 1% for P waves and 2% for S waves of *Zamora* [1990]. Although no information about the accuracy of the densities is available in the aforementioned references, we assume it better than 1%. If this assumption is true, the estimated accuracies of the SOE and TOE constants are better than 5% and 15%, respectively.

The results showing SOE and TOE coefficients are listed in Table 1. For comparison we have also listed the results for "intact" homogeneous media, such as iron and Pyrex [*Hughes and Kelly*, 1953]. The predicted and measured values of the

Table 1. Second- and Third-Order Moduli and Predicted and Measured Parameters in Rocks Compared With Sample Materials Without Mechanical Defects

		Elastic Constants					Predicted and Measured Elastic Parameters				
		Second Order (Usual Elastic)		Third Order (Murnaghan Coefficients)			b_S, GPa^{-1}		a_P, GPa^{-1}		
Materials	ρ, kg/m^3	K, GPa	μ, GPa	l, GPa	m, GPa	n, GPa	Pred.	Meas.	Pred.	Meas.	β
					Hughes and Kelly [1953]						
Armco iron		164	82	−348	−1,030	1,100	0.027		0.032		7.3
Pyrex		31.8	27.5	14	92	420	0.088		0.092		4.4
					Nur and Simmons [1969]						
Barre granite	2650	13.8	18.2	−3,371	−6,742	−6,600	−2.47	−2.47	−9.67	−8.66	−441
					Zamora [1990]						
Dry F32 Fontainebleau sandstone	2414	15.3	11.7	−97,800	−99,400	−84,900	−77.2	−71.9	−274		−9,600
Dry F32, thermally cracked	2414	7.8	5.7	−74,000	−64,500	−34,900	−136	−134	−740		−13,200
Water-Saturated F32, thermally cracked	2503	30.2	17.5	−59,100	−38,200	−27,500	−9.4	−9.3	−35.8		−2,430
Dry D82 marble	2870	30	21.3	−40,300	−35,400	−20,300	−5.5	−5.5	−28.3		−1,900

Here, ρ is density; K and μ are second-order bulk and shear moduli, respectively; l, m, and n are defined in text; b_S and a_P are stress-induced S wave birefringence and P wave anisotropy coefficients, respectively; and β is nonlinear acoustic coefficient (equation (8)). Pred., predicted; Meas., measured.

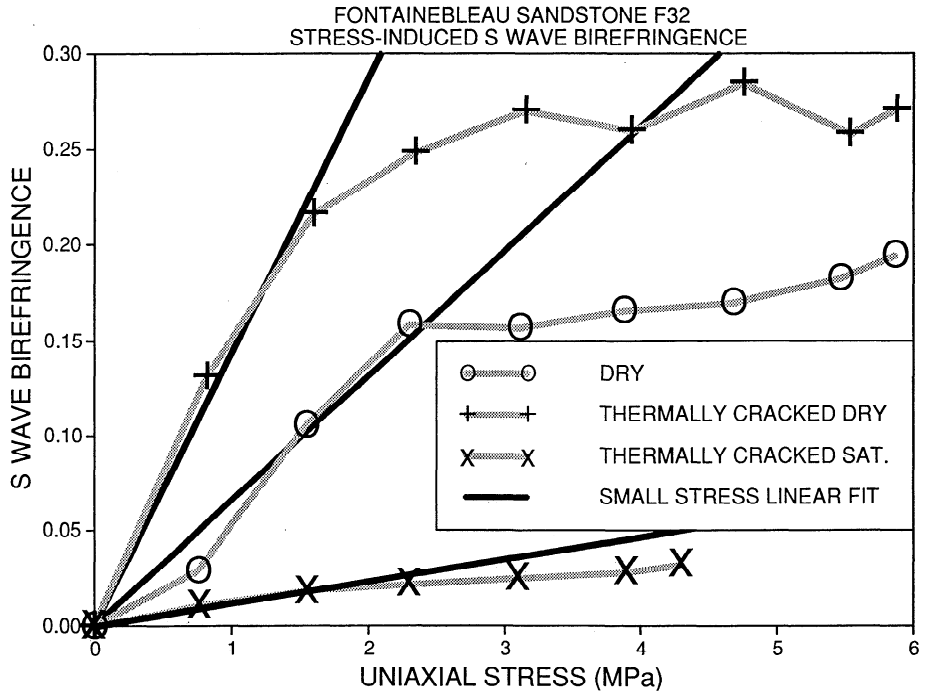

Figure 3. S wave birefringence B_S as function of the uniaxial stress in "natural" and "thermally cracked" Fontainebleau sandstone, both dry and saturated. Direction of propagation is perpendicular to the stress. Experimental data are from *Zamora* [1990]. Theoretical results from equation (22) (with $\theta = \pi/2$) are shown as solid line.

stress-induced S wave birefringence coefficient b_S (see (22)) and the stress-induced P wave anisotropy coefficient a_P (see (25)) are also shown. Finally, the predicted value of the nonlinear acoustic coefficient β from (8) is reported.

From (13) one can deduce the order of magnitude of the maximum stress below which the proportionality between the relative variation $[M(\sigma) - M(\sigma = 0)]/M(\sigma = 0)$ of the wave modulus and the applied stress σ, described by (12), is a good approximation. Using (13) and the data of Table 1, this leads to small limiting stresses of the order of a few megapascals or fractions of a megapascal for strongly nonlinear materials such as thermally cracked, dry Fontainebleau sandstone. From the experimental data plotted in Figures 2, 3 and 4 it appears that the relations of proportionality are still reasonable for much larger stress levels, suggesting limiting stresses at least one order of magnitude larger than those predicted theoretically from (13).

Figure 3 shows the variation of the S birefringence as a function of the applied uniaxial stress in Fontainebleau sandstone. The linear fit between the S birefringence and the stress, described by (19) and plotted as solid lines in Figure 3, is reasonable for stress levels that are not too high. The same observations stand for the P anisotropy in Barre granite in Figure 4.

In regard to the relative variations of $\gamma = V_P/V_S$ with hydrostatic pressure (Figure 5), the proportionality relationship described by (27) and illustrated by the solid line in Figure 5 becomes rapidly unsatisfactory even for moderate pressures (typically larger than 10 MPa) and for rocks exhibiting weak nonlinearity as is the case for Brauvilliers limestone. In other words, the domain of validity of this equation is restricted to a much smaller pressure range (typically a factor of 10 or less) than for (22) and (25). In spite of the noisiness of the data, we believe that the decrease of γ with pressure, although weak, is consistent with crack closure [e.g., *Wilkens et al.*, 1984].

From data of *Nur and Simmons* [1969] it is possible to analyze the stress-induced velocity variations for intermediate directions of propagation, θ. Figure 6 shows the dependence of the stress derivative $[\partial(\rho_0 W^2)/\partial\sigma]_{\sigma=0}$ of the P, SV, and SH wave moduli on θ in Barre granite (see (9), (14), (15) and (16)). The P wave exhibits a much larger variation of the stress derivative of modulus with direction of propagation than does the SH wave. The larger pressure dependence of the moduli/velocities is observed in the direction parallel to the direction of the stress, and vice versa. Note that in contrast, the stress derivative of the SV wave modulus is practically independent of the direction of propagation, which is confirmed by theory (see Table 1 and equations (9) and (15), where the term H_{SV}, independent of the direction of propagation, is orders of magnitude larger than the other terms on the right-hand side of (9)). In fact, this is a general result in strongly nonlinear isotropic media such as rocks that can be considered as isotropic in the unstressed condition; however, it is not true in weakly nonlinear media, such as crystals, where "geometrical" nonlinearity and "physical" nonlinearity are of comparable order of magnitude [*Rasolofosaon and Yin*, 1995].

A simple way to check the validity of (22) and (25) exhibiting a simple angular dependence of the S-birefringence $B_S(\theta)$ and the P-anisotropy $A_P(\theta)$ in $\sin^2\theta$, is to plot the normalized values $B_S(\theta)/B_S(\theta = 90°)$ and $A_P(\theta)/A_P(\theta = 90°)$ of these quantities as a function of the direction of propagation θ. This is done in Figure 7 for Barre granite under uniaxial stress. The experimental data are compared with the theoretical prediction of $\sin^2\theta$. The agreement between experiment and theory is satisfactory for P wave anisotropy, but not so for the S birefringence. There are at least two possible explanations for

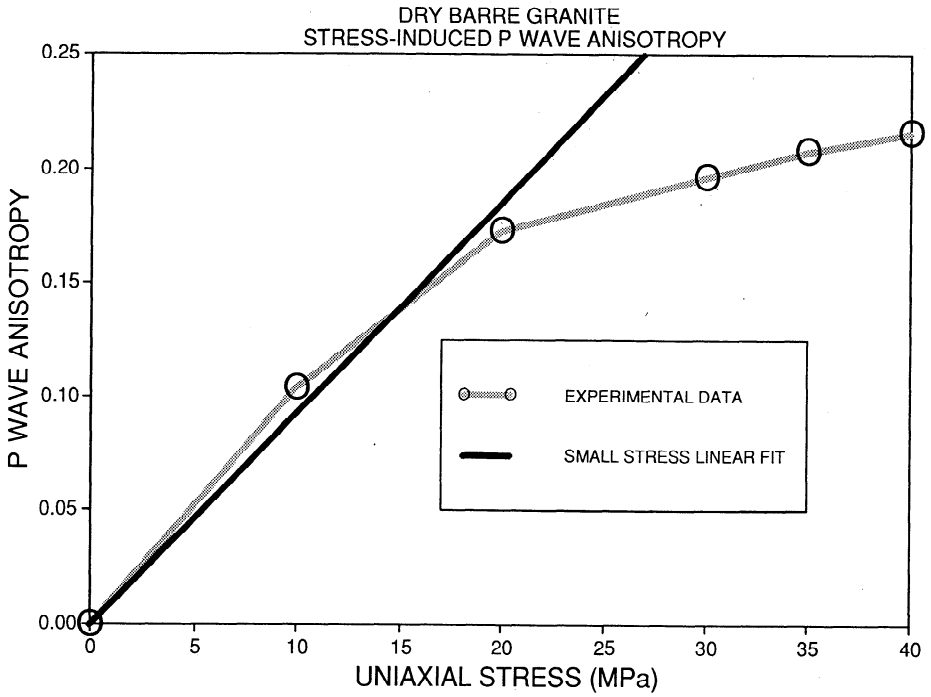

Figure 4. P wave anisotropy A_P as function of the uniaxial stress in dry Barre granite. Experimental data are from *Nur and Simmons* [1969]. Theoretical results from equation (25) (with $\theta - \pi/2$) are shown as solid line.

this result. First, the stress-induced S birefringence is much smaller than the stress-induced P anisotropy (see Table 1 and Figure 6), which seems to be true for all rocks shown in Table 1. Second, the S velocities are practically much more difficult to measure than P velocities [e.g., *Bourbié et al.*, 1987]. Taken together, these two explanations imply that the error bars for the S wave in Figure 7 must be much larger than those for the P wave.

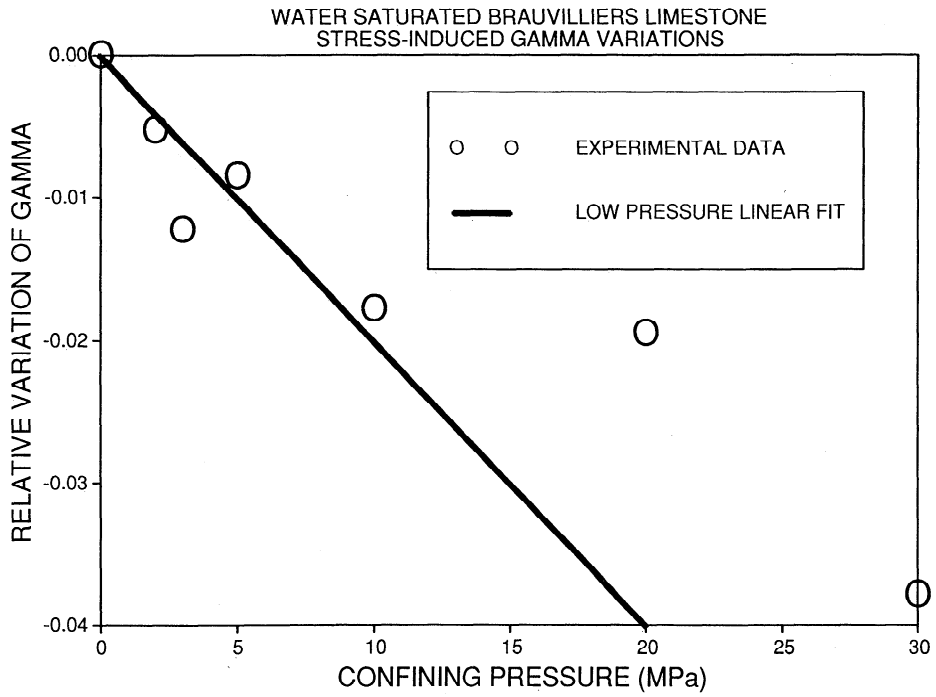

Figure 5. Relative variation $\Delta\gamma/\gamma$ of $\gamma = V_P/V_S$ as a function of the confining pressure in water-saturated Brauvilliers limestone. Experimental data are from *Lucet* [1989]. Theoretical results from equation (27) are shown as solid line.

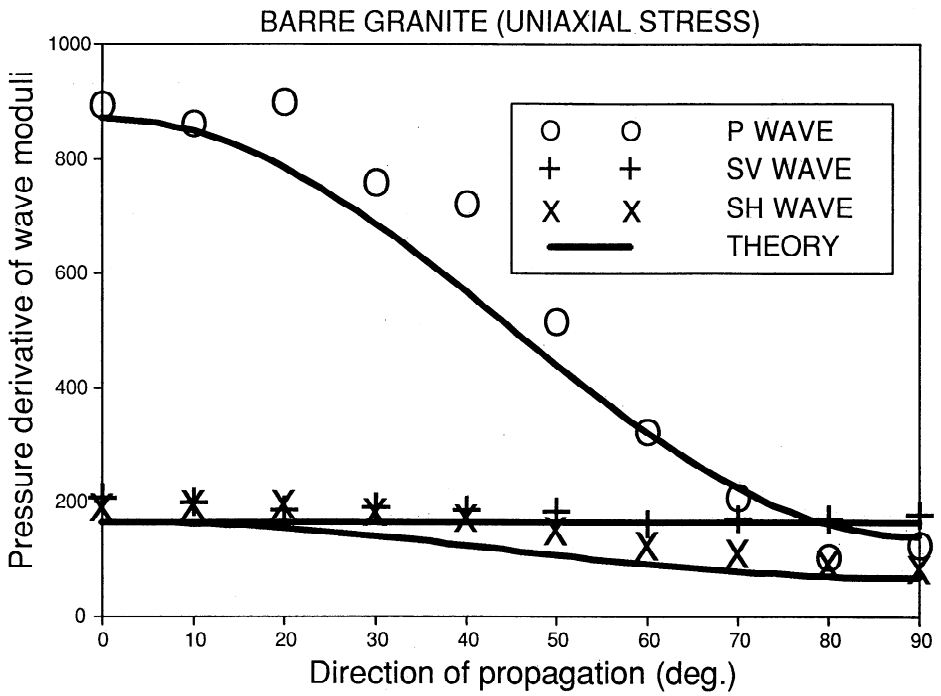

Figure 6. Dependence of the pressure derivatives of the P wave, the SV wave, and the SH wave moduli on the direction of propagation with respect to the direction of the applied uniaxial stress in dry Barre granite. Experimental data are from *Nur and Simmons* [1969]. Theoretical results from equations (9), (14), (15), and (16) are shown as solid lines.

Discussion

A key point in our reasoning for the inversion of the TOE constants is that we attribute all the stress-induced anisotropy to the pressure dependence of the velocities under anisotropic applied stress, or, in other words, to the presence of nonlinearity in rocks. Thus a natural question arises. Because most rocks are anisotropic to some degree in a SOE sense, what is the influence of the SOE anisotropy of the unstressed rock on

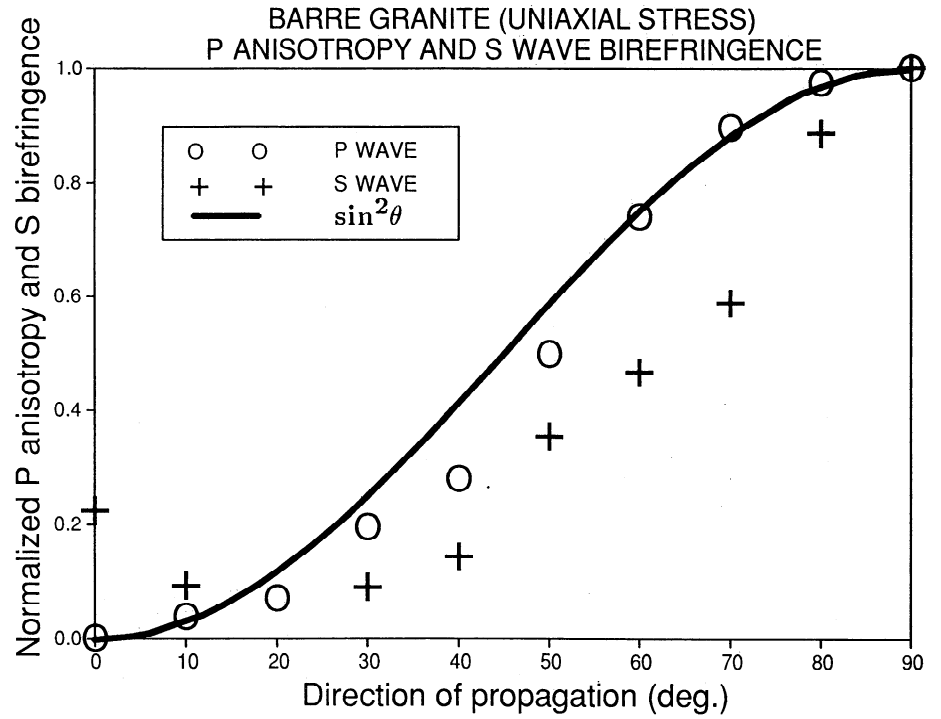

Figure 7. Dependence of the normalized P anisotropy $(A_P(\theta)/A_P(\theta = \pi/2))$ and S-birefringence $(B_S(\theta)/B_S(\theta = \pi/2))$ on the direction of propagation, θ, in dry Barre granite. Experimental data are from *Nur and Simmons* [1969]. The in solid line is $\sin^2\theta$.

the determination of the TOE constants? In fact, the SOE anisotropy has a relatively minor influence in the inversion procedure of the TOE constants, primarily because the inversion of these constants is practically decoupled from the inversion of the SOE constants. The SOE inversion is based only on the unstressed moduli measurements and consists in searching for the "best isotropic medium" which approximates the unstressed rock. On the other hand, the TOE inversion is based not on stress-induced anisotropy measurements but on measurements of the stress-derivatives of the wave moduli (see (9)). In the case of strongly nonlinear materials such as rock (see comments after (11)), stress derivatives are clearly dominated by the presence of the TOE constants in the H term of (9), with the SOE constants playing a relatively minor role. In fact, in the TOE inversion one should be more concerned about the TOE anisotropy than about the SOE anisotropy because the TOE seems always to be much larger than TOE in rocks and their constituent minerals [*Rasolofosaon and Yin*, 1995]. An illustration of the relevancy of the proposed procedure is the surprisingly good agreement between the directly measured stress-induced S birefringence and P anisotropy coefficients, b_S and a_P, respectively, and the predicted values deduced from the inverted SOE and TOE constants using (22) and (25) (see Table 1). It is worth noting that the parameters reported in Table 1 quantify the stress-induced effects per unit of applied stress and not the global stress-induced effects themselves. This minimizes the bias induced the presence of SOE anisotropy, which is by definition independent of the stress level.

In regard to the anisotropy induced by an arbitrary state of stress in an initially isotropic medium (see (12)), there are few examples of such data in the literature. *Nur and Simmons* [1969] studied P wave propagation in Barre granite under various states of biaxial stress. Their Figure 10 showing P wave isovelocity diagrams is identical to traces of the plane π in the coordinate plane (I, II) for different values of the projection Σ_Δ (see Figure 1). This observation provides an approximate confirmation of the theory. Note than in the case of an initially isotropic medium the gradient vector is collinear to the direction (1, 1, 1). As a consequence, the isovelocity lines in the plane (I, II) should be straight lines perpendicular to the first bisector of the axes I and II in Figure 1. This prediction is approximately corroborated by the data from Nur and Simmons. Nevertheless, in detail their results show that the stress derivative of the P velocity in the direction I is roughly 1.5 times larger than that in direction II, whereas the P velocities in these directions are practically identical. This certainly implies that Barre granite is more anisotropic with respect to the TOE properties than with respect to SOE properties, which is in agreement with the conclusions of *Rasolofosaon and Yin* [1995].

It is clear from Table 1 that the TOE constants in rock are 2 or 3 orders of magnitude larger than the SOE constants and differ in sign. The magnitude of the nonlinear response, quantified by β in (8), is orders of magnitude larger in the rock samples than in the "intact" materials iron and Pyrex. It is also clear that this ratio increases by 1 order of magnitude when dry Fontainebleau sandstone is thermally cracked, whereas the velocities, or the square root of the SOE constants, increase by less than a factor of 2. This was also observed by *Zinov'yeva et al.* [1989] in siltstone. It is not surprising that the thermal cracking of the sample increases the pressure dependence (see Figure 2). On the other hand, the presence of a saturating liquid (water) in the cracks reduces the contrast between the matrix and the crack properties, which has the same effect as reducing the crack density. As a consequence, the pressure dependence is strongly reduced, at least for the P waves.

As is shown in Table 1, it is clear that "physical" nonlinearity strongly dominates over "geometrical" nonlinearity in rock, whereas they play a comparable role in iron and Pyrex. Similar results in anisotropic rocks compared to crystals and liquids are reported by *Rasolofosaon and Yin* [1995]. We and other researchers have measured large values of β in granite, sandstones, and limestones [e.g., *Bakulin and Protosenya*, 1982; *Meegan et al.*, 1993; *Johnson et al.*, 1993].

All the TOE constants are negative in the rocks measured, but this appears to be fortuitous [e.g., *Bakulin and Protosenya*, 1982; *Nazarov et al.*, 1988; *Rasolofosaon and Yin*, 1995]. Therefore inspection of (18), (19), and (20) implies that in general, rock velocities increase with pressure. Numerous observations in the literature support this well-known fact. On the other hand, velocity may decrease with pressure in some materials, for example, Pyrex.

The relationship is clear between the "amount" of nonlinearity in the rock, quantified, for example, by the magnitude of the nonlinear coefficient β in Table 1, and the "intensity" of the stress-induced anisotropy, quantified by the S wave birefringence or P wave anisotropy coefficients b_S and a_P, respectively. In "intact" homogeneous media the coefficients b_S and a_P do not exceed 0.1 GPa^{-1}, and β remains small in absolute value and can be either positive or negative. In rocks these coefficients are all negative and are larger by 1–4 orders of magnitude, meaning that nonlinear elasticity and stress-induced S birefringence and P anisotropy are much larger in rocks than in "intact" homogeneous materials. Furthermore, the effect on rock is always in the same manner. For example, in the presence of uniaxial stress and for wave propagation in a direction perpendicular to the direction of stress, the fast shear wave S_1 and the slow shear wave S_2 are always polarized parallel and perpendicular to the direction of the applied stress, respectively. Notice that it is exactly the opposite in the case of iron and Pyrex. For P anisotropy in rocks under uniaxial pressure, the P wave propagating in the direction of the applied stress always propagates faster than the one propagating perpendicular to that direction. Iron exhibits the same behavior, whereas Pyrex exhibits the opposite. Note also that in all rocks, the stress-induced P wave anisotropy is much larger than the stress-induced S wave birefringence (see Figure 5 and the values of a_P and b_S in Table 1).

Conclusions

In this paper we have developed the relationship between the nonlinear elastic parameters of rocks and the stress-induced effects on waves propagating in rocks, in this case, transverse isotropy induced by uniaxial stress. We demonstrated first that the stress-induced P anisotropy and S birefringence are proportional to the applied uniaxial stress σ, second that their directional dependence is governed by the unique function $\sin^2\theta$ (θ being the angle between the direction of propagation and the direction of the uniaxial stress), and third that the constant of proportionality is a ratio of polynomial functions of the linear and the nonlinear elastic constants.

We have also quantified the linear elastic constants, or Lamé

parameters, and the nonlinear elastic constants, or Murnaghan coefficients, for experimental data available in the literature. We show that knowledge of the complete set of these elastic constants allows one to predict the stress-induced variations of the modulus of whatever wave type propagating in an arbitrary direction in a rock submitted to an arbitrary (but uniform) state of stress.

Contrary to "intact" homogeneous solids (iron, Pyrex), rocks can exhibit strong nonlinearity ("physical" nonlinearity always dominating "geometrical" nonlinearity) and always in the same manner (i.e., an increase of the moduli with pressure). As a consequence, the stress-induced P anisotropy and S birefringence can be large for an isotropic material subjected to uniaxial stress. From a quantitative point of view, for these types of experiments the agreement between the theoretical predictions and the experimental results is good.

We suggest that future experiments on nonlinear elasticity in rocks be conducted in order (1) to check the generality of our results, (2) to show unambiguously the detectability of the nonlinear effects in rocks, and (3) to demonstrate the relevancy of such properties for geophysical purposes. Different forms of anisotropy from different states and initially anisotropic rocks should be examined in the future as well [e.g., *Yin and Rasolofosaon*, 1994; *Rasolofosaon and Yin*, 1995]. In order to keep the paper a reasonable length, the relation between the nonlinear parameters and specific micromechanical models [e.g., *Palciauskas*, 1992; *Tutuncu and Sharma*, 1994; *Schwartz et al.*, 1994] has not been described here, but will be studied in future work. Finally, we are fully aware that hysteresis and discrete memory effects can contribute dramatically to the nonlinear response of a material as illustrated by *McCall and Guyer* [1994] and *Guyer et al.* [1994, 1995]. In future work, these effects must be accounted for.

Acknowledgments. This research is a result of a scientific collaboration between the Geological Engineering Group of Los Alamos National Laboratory, under D.O.E. Office of Basic Energy Science contract W7404-ENG-36, and the Rock Physics Laboratory of the Institut Français du Pétrole (France). We gratefully acknowledge M. Zamora, from the Institut de Physique du Globe of Paris (France), for allowing us to use her experimental data, and A. Zarembowitch, from the Université Pierre et Marie Curie (France), and B. Zinszner, from the Institut Français du Pétrole (France), for fruitful and illuminating discussions. We also wish to thank P. A. Berge, from Lawrence Livermore National Laboratory; T. Duffy, from Carnegie Institute of Washington; and an anonymous reviewer for their helpful comments.

References

Bakulin, V. N., and A. G. Protosenya, Nonlinear effects in travel of elastic waves through rocks (in Russian), *Dokl. Akad. Nauk SSSR*, *2*, 314–316, 1982.

Beyer, R. T., Nonlinear acoustics (Experimental), in *American Institute of Physics Handbook*, edited by D. E. Gray, pp. 3.206–3.210, McGraw-Hill, New York, 1972.

Birch, F., Compressibility; elastic constants, in *Handbook of Physical Constants*, edited by S. P. Clark Jr., *Mem. Geol. Soc. Am.*, *97*, 97–174, 1966.

Bourbié, T., O. Coussy, and B. E. Zinszner, *Acoustics of Porous Media*, Gulf, Houston, Texas, 1987.

Brugger, K., Thermodynamic definition of higher order elastic coefficients, *Phys. Rev. A 133*, 1611–1612, 1964.

Brugger, K., Pure mode for elastic waves in crystals, *J. Appl. Phys.*, *36*, 759–768, 1965.

Crampin, S., and J. H. Lovell, A decade of shear-wave splitting in the Earth's crust: What does it mean? and what should we do next?, *Geophys. J. Int.*, *107*, 387–407, 1991.

Curie, M., *Pierre Curie* (in French), Denoel, Paris, 1955.

Curie, P., Sur la symétric dans les phénomènes physiques, symétrie d'un champ éléctrique et d'un champ magnétique, *J. Phys., Ser. 3, III*, 393–415, 1894.

Gol'dberg, Z. A., On the propagation of plane waves of finite amplitude, *Sov. Phys. Acoust.*, Engl. Transl., *3*, 340–347, 1957.

Green, R. E., Jr., *Ultrasonic Investigation of Mechanical Properties*, Academic, San Diego, Calif., 1973.

Guyer, R. A., K. R. McCall, and G. N. Boitnott, Hysteresis, discrete memory, and nonlinear wave propagation in rock, *Phys. Rev. Lett.*, *74*, 3491–3494, 1994.

Guyer, R. A., K. R. McCall, P. A. Johnson, P. N. J. Rasolofosaon, and B. E. Zinszner, Equation of state hysteresis and resonant bar measurements on rocks, *U.S. Symp. Rock Mech.*, *35th*, 177–181, 1995.

Hamilton, M. F., Fundamentals and applications of nonlinear acoustics, in *Nonlinear Wave Propagation in Mechanics*, edited by T. W. Wright, pp. 1–28, Am. Soc. of Mech. Eng., New York, 1986.

Hearmon, R. F. S., *An Introduction to Applied Anisotropic Elasticity*, Oxford Univ. Press, New York, 1961.

Helbig, K., *Foundations of Anisotropy for Exploration Seismics*, Pergamon, Tarrytown, New York, 1994.

Hughes, D. S., and J. L. Kelly, Second-order elastic deformation of solids, *Phys. Rev.*, *92*, 1145–1149, 1953.

Jaeger, J. C., and N. G. W. Cook, *Fundamentals of Rock Mechanics*, 3rd ed., Chapman and Hall, London, 1979.

Johnson, P. A., and K. R. McCall, Observation and implications of nonlinear elastic wave response in rock, *Geophys. Res. Lett.*, *21*, 165–168, 1994.

Johnson, P. A., P. N. J. Rasolofosaon, and B. E. Zinszner, Measurement of nonlinear elastic response in rock by the resonant bar method, in *Advances in Nonlinear Acoustics*, edited by H. Hobaek, pp. 531–536, World Sci., Singapore, 1993.

Kostek, S., B. K. Sinha, and A. N. Norris, Third-order elastic constants for an inviscid fluid, *J. Acoust. Soc. Am.*, *94*, 3014–3017, 1993.

Leary, P. C., S. Crampin, and T. V. McEvilly, Seismic fracture anisotropy in the Earth's crust, *J. Geophys. Res.*, *95*, 11,105–11,114, 1990.

Lucet, N., Velocity and attenuation of sonic and ultrasonic waves in rocks under confining pressure (in French), Ph.D. thesis, Univ. of Paris VI, Paris, 1989.

McCall, K. R., and R. A. Guyer, Equation of state and wave propagation in hysteretic nonlinear elastic materials, *J. Geophys. Res.*, *99*, 23,887–23,897, 1994.

Meegan, G. D., Jr., P. A. Johnson, R. A. Guyer, and K. R. McCall, Observations of nonlinear elastic wave behavior in sandstones, *J. Acoust. Soc. Am.*, *94*, 3387–3391, 1993.

Murnaghan, F. D., *Finite Deformation of an Elastic Solid*, John Wiley, New York, 1951.

Nazarov, V. E., L. A. Ostrovsky, I. A. Soustova, and A. M. Soutin, Nonlinear acoustics of micro-inhomogeneous media, *Phys. Earth Planet. Inter.*, *50*, 65–73, 1988.

Nur, A., Effects of stress on velocity anisotropy in rocks with cracks, *J. Geophys. Res.*, *76*, 2022–2034, 1971.

Nur, A., and G. Simmons, Stress-induced velocity anisotropy in rock, *J. Geophys. Res.*, *74*, 6667–6674, 1969.

Palciauskas, V. V., Compressional to shear wave velocity ratio of granular rocks: Role of rough grain contacts, *Geophys. Res. Lett.*, *19*, 1683–1686, 1992.

Pao, Y. H., W. Sachse, and H. Fukuoka, Acoustoelasticity and ultrasonic measurements of residual stresses, *Phys. Acoust.*, *17*, 61–143, 1984.

Pickett, G. R., Acoustic character logs and their applications in formation evaluation, *J. Pet. Technol.*, *15*, 650–667, 1963.

Rasolofosaon, P. N. J., and H. Yin, Simultaneous characterization of anisotropy and nonlinearity in arbitrary elastic media—Reflections on experimental data, in *Transactions of the 6th International Workshop on Seismic Anisotropy*, Soc. of Explor. Geophys., Tulsa, Okla., in press, 1995.

Schwartz, L. M., W. F. Murphy, and J. G. Berryman, Stress-induced transverse isotropy in rocks (abstract), *SEG 64th Annual Meeting Technical Program (Los Angeles CA), Expanded Abstracts*, pap. SL1.7, 1081–1085, Soc. of Explor. Geophys., Tulsa, Okla., 1994.

Sirotine, Y. I., and M. P. Chaskolskaya, *Fundamentals of Crystal Physics* (in Russian), Nauka, Moscow, 1975.

Thurston, R. N., and K. Brugger, Third-order elastic constants and the velocity of small amplitude elastic waves in homogeneously stressed media, *Phys. Rev. A*, *133*, 1604–1610, 1964.

Truesdell, C., *Problems of Nonlinear Elasticity*, Gordon and Breach, New York, 1965.

Tutuncu, A. N., and M. M. Sharma, The influence of grain contact stiffness and frame moduli in sedimentary rocks, *Geophysics*, *57*, 1571–1582, 1992.

Walsh, J. B., The effect of cracks on the compressibility of rock, *J. Geophys. Res.*, *70*, 381–383, 1965.

Wilkens, R., G. Simmons, and L. Caruso, The ratio V_P/V_S as a discriminant of composition of siliceous limestones, *Geophysics*, *49*, 1850–1860, 1984.

Yin, H., and P. N. J. Rasolofosaon, Nonlinear and linear elastic behavior of anisotropic rocks: Ultrasonic experiments versus theoretical predictions, in *SEG 64th Annual Meeting Technical Program (Los Angeles CA), Expanded Abstracts*, pap. SL3.4, pp. 1129–1132, Soc. of Explor. Geophys., Tulsa, Okla., 1994.

Zamora, M., Experimental study of the effect of the geometry of rock porosity on the velocities of elastic waves (in French), Docteur ès Sciences thesis, Univ. of Paris VII, Paris, 1990.

Zarembo, L. K., and V. A. Krasil'nikov, Nonlinear phenomena in the propagation of elastic waves in solids, *Sov. Phys. Usp.*, Engl. Transl., *13*, 778–797, 1971.

Zinov'yeva, G. P., I. I. Nesterov, L. Zhdakhin, E. E. Artma, and Y. U. Gorbunov, Investigation of rock deformation properties in terms of the nonlinear acoustic parameter (in Russian), *Dokl. Akad. Nauk SSSR*, *307*, 337–341, 1989.

Zoback, M. L., First- and second-order patterns of stress in the lithosphere: The World Stress Map project, *J. Geophys. Res.*, *97*, 11,703–11,728, 1992.

P. A. Johnson, Geological Engineering Group, Earth and Environmental Sciences Division, Mail Stop D443, Los Alamos National Laboratory, Los Alamos, NM 87545. (e-mail: johnson@seismo5.lanl.gov)

P. N. J. Rasolofosaon, Institut Français du Pétrole, B.P. 311, 92506 Rueil Malmaison Cedex, France. (e-mail: patrick.rasolofosaon@ifp.fr)

(Received January 31, 1995; revised May 5, 1995;
accepted September 15, 1995.)